

Common Suppression Pattern of η and π^0 Mesons at High Transverse Momentum in Au + Au Collisions at $\sqrt{s_{NN}} = 200$ GeV

S. S. Adler,⁵ S. Afanasiev,¹⁸ C. Aidala,⁵ N. N. Ajitanand,⁴⁴ Y. Akiba,^{21,39} J. Alexander,⁴⁴ R. Amirikas,¹² L. Aphecetche,⁴⁶ S. H. Aronson,⁵ R. Averbeck,⁴⁵ T. C. Awes,³⁶ R. Azmoun,⁴⁵ V. Babintsev,¹⁵ A. Baldisseri,¹⁰ K. N. Barish,⁶ P. D. Barnes,²⁸ B. Bassalleck,³⁴ S. Bathe,³¹ S. Batsouli,⁹ V. Baublis,³⁸ A. Bazilevsky,^{40,15} S. Belikov,^{17,15} Y. Berdnikov,⁴¹ S. Bhagavatula,¹⁷ J. G. Boissevain,²⁸ H. Borel,¹⁰ S. Borenstein,²⁶ M. L. Brooks,²⁸ D. S. Brown,³⁵ N. Bruner,³⁴ D. Bucher,³¹ H. Buesching,³¹ V. Bumazhnov,¹⁵ G. Bunce,^{5,40} J. M. Burward-Hoy,^{27,45} S. Butsyk,⁴⁵ X. Camard,⁴⁶ J.-S. Chai,¹⁹ P. Chand,⁴ W. C. Chang,² S. Chernichenko,¹⁵ C. Y. Chi,⁹ J. Chiba,²¹ M. Chiu,⁹ I. J. Choi,⁵³ J. Choi,²⁰ R. K. Choudhury,⁴ T. Chujo,⁵ V. Cianciolo,³⁶ Y. Cobigo,¹⁰ B. A. Cole,⁹ P. Constantin,¹⁷ D. d'Enterria,⁴⁶ G. David,⁵ H. Delagrange,⁴⁶ A. Denisov,¹⁵ A. Deshpande,⁴⁰ E. J. Desmond,⁵ A. Devismes,⁴⁵ O. Dietzsch,⁴² O. Drapier,²⁶ A. Drees,⁴⁵ R. du Rietz,³⁰ A. Durum,¹⁵ D. Dutta,⁴ Y. V. Efremenko,³⁶ K. El Chenawi,⁵⁰ A. Enokizono,¹⁴ H. En'yo,^{39,40} S. Esumi,⁴⁹ L. Ewell,⁵ D. E. Fields,^{34,40} F. Fleuret,²⁶ S. L. Fokin,²⁴ B. D. Fox,⁴⁰ Z. Fraenkel,⁵² J. E. Frantz,⁹ A. Franz,⁵ A. D. Frawley,¹² S.-Y. Fung,⁶ S. Garpman,^{30,*} T. K. Ghosh,⁵⁰ A. Glenn,⁴⁷ G. Gogiberidze,⁴⁷ M. Gonin,²⁶ J. Gosset,¹⁰ Y. Goto,⁴⁰ R. Granier de Cassagnac,²⁶ N. Grau,¹⁷ S. V. Greene,⁵⁰ M. Grosse Perdekamp,⁴⁰ W. Guryn,⁵ H.-Å. Gustafsson,³⁰ T. Hachiya,¹⁴ J. S. Haggerty,⁵ H. Hamagaki,⁸ A. G. Hansen,²⁸ E. P. Hartouni,²⁷ M. Harvey,⁵ R. Hayano,⁸ N. Hayashi,³⁹ X. He,¹³ M. Heffner,²⁷ T. K. Hemmick,⁴⁵ J. M. Heuser,⁴⁵ M. Hibino,⁵¹ H. Hiejima,¹⁶ J. C. Hill,¹⁷ W. Holzmann,⁴⁴ K. Homma,¹⁴ B. Hong,²³ A. Hoover,³⁵ T. Ichihara,^{39,40} V. V. Ikonnikov,²⁴ K. Imai,^{25,39} D. Isenhower,¹ M. Ishihara,³⁹ M. Issah,⁴⁴ A. Isupov,¹⁸ B. V. Jacak,⁴⁵ W. Y. Jang,²³ Y. Jeong,²⁰ J. Jia,⁴⁵ O. Jinnouchi,³⁹ B. M. Johnson,⁵ S. C. Johnson,²⁷ K. S. Joo,³² D. Jouan,³⁷ S. Kametani,^{8,51} N. Kamihara,^{48,39} J. H. Kang,⁵³ S. S. Kapoor,⁴ K. Katou,⁵¹ S. Kelly,⁹ B. Khachaturov,⁵² A. Khanzadeev,³⁸ J. Kikuchi,⁵¹ D. H. Kim,³² D. J. Kim,⁵³ D. W. Kim,²⁰ E. Kim,⁴³ G.-B. Kim,²⁶ H. J. Kim,⁵³ E. Kistenev,⁵ A. Kiyomichi,⁴⁹ K. Kiyoyama,³³ C. Klein-Boesing,³¹ H. Kobayashi,^{39,40} L. Kochenda,³⁸ V. Kochetkov,¹⁵ D. Koehler,³⁴ T. Kohama,¹⁴ M. Kopytine,⁴⁵ D. Kotchetkov,⁶ A. Kozlov,⁵² P. J. Kroon,⁵ C. H. Kuberg,^{1,28,*} K. Kurita,⁴⁰ Y. Kuroki,⁴⁹ M. J. Kweon,²³ Y. Kwon,⁵³ G. S. Kyle,³⁵ R. Lacey,⁴⁴ V. Ladygin,¹⁸ J. G. Lajoie,¹⁷ A. Lebedev,^{17,24} S. Leckey,⁴⁵ D. M. Lee,²⁸ S. Lee,²⁰ M. J. Leitch,²⁸ X. H. Li,⁶ H. Lim,⁴³ A. Litvinenko,¹⁸ M. X. Liu,²⁸ Y. Liu,³⁷ C. F. Maguire,⁵⁰ Y. I. Makdisi,⁵ A. Malakhov,¹⁸ V. I. Manko,²⁴ Y. Mao,^{7,39} G. Martinez,⁴⁶ M. D. Marx,⁴⁵ H. Masui,⁴⁹ F. Matathias,⁴⁵ T. Matsumoto,^{8,51} P. L. McGaughey,²⁸ E. Melnikov,¹⁵ F. Messer,⁴⁵ Y. Miake,⁴⁹ J. Milan,⁴⁴ T. E. Miller,⁵⁰ A. Milov,^{45,52} S. Mioduszewski,⁵ R. E. Mischke,²⁸ G. C. Mishra,¹³ J. T. Mitchell,⁵ A. K. Mohanty,⁴ D. P. Morrison,⁵ J. M. Moss,²⁸ F. Mühlbacher,⁴⁵ D. Mukhopadhyay,⁵² M. Muniruzzaman,⁶ J. Murata,^{39,40} S. Nagamiya,²¹ J. L. Nagle,⁹ T. Nakamura,¹⁴ B. K. Nandi,⁶ M. Nara,⁴⁹ J. Newby,⁴⁷ P. Nilsson,³⁰ A. S. Nyanin,²⁴ J. Nystrand,³⁰ E. O'Brien,⁵ C. A. Ogilvie,¹⁷ H. Ohnishi,^{5,39} I. D. Ojha,^{50,3} K. Okada,³⁹ M. Ono,⁴⁹ V. Onuchin,¹⁵ A. Oskarsson,³⁰ I. Otterlund,³⁰ K. Oyama,⁸ K. Ozawa,⁸ D. Pál,⁵² A. P. T. Palounek,²⁸ V. Pantuev,⁴⁵ V. Papavassiliou,³⁵ J. Park,⁴³ A. Parmar,³⁴ S. F. Pate,³⁵ T. Peitzmann,³¹ J.-C. Peng,²⁸ V. Peresedov,¹⁸ C. Pinkenburg,⁵ R. P. Pisani,⁵ F. Plasil,³⁶ M. L. Purschke,⁵ A. K. Purwar,⁴⁵ J. Rak,¹⁷ I. Ravinovich,⁵² K. F. Read,^{36,47} M. Reuter,⁴⁵ K. Reygers,³¹ V. Riabov,^{38,41} Y. Riabov,³⁸ G. Roche,²⁹ A. Romana,^{26,*} M. Rosati,¹⁷ P. Rosnet,²⁹ S. S. Ryu,⁵³ M. E. Sadler,¹ B. Sahlmueller,³¹ N. Saito,^{39,40} T. Sakaguchi,^{8,51} M. Sakai,³³ S. Sakai,⁴⁹ V. Samsonov,³⁸ L. Sanfratello,³⁴ R. Santo,³¹ H. D. Sato,^{25,39} S. Sato,^{5,49} S. Sawada,²¹ Y. Schutz,⁴⁶ V. Semenov,¹⁵ R. Seto,⁶ M. R. Shaw,^{1,28} T. K. Shea,⁵ T.-A. Shibata,^{48,39} K. Shigaki,^{14,21} T. Shiina,²⁸ C. L. Silva,⁴² D. Silvermyr,^{28,30} K. S. Sim,²³ C. P. Singh,³ V. Singh,³ M. Sivertz,⁵ A. Soldatov,¹⁵ R. A. Soltz,²⁷ W. E. Sondheim,²⁸ S. P. Sorensen,⁴⁷ I. V. Sourikova,⁵ F. Staley,¹⁰ P. W. Stankus,³⁶ E. Stenlund,³⁰ M. Stepanov,³⁵ A. Ster,²² S. P. Stoll,⁵ T. Sugitate,¹⁴ J. P. Sullivan,²⁸ E. M. Takagui,⁴² A. Taketani,^{39,40} M. Tamai,⁵¹ K. H. Tanaka,²¹ Y. Tanaka,³³ K. Tanida,³⁹ M. J. Tannenbaum,⁵ P. Tarján,¹¹ J. D. Tepe,^{1,28} T. L. Thomas,³⁴ J. Tojo,^{25,39} H. Torii,^{25,39} R. S. Towell,¹ I. Tserruya,⁵² H. Tsuruoka,⁴⁹ S. K. Tuli,³ H. Tydesjö,³⁰ N. Tyurin,¹⁵ H. W. van Hecke,²⁸ J. Velkovska,^{5,45} M. Velkovsky,⁴⁵ V. Veszprémi,¹¹ L. Villatte,⁴⁷ A. A. Vinogradov,²⁴ M. A. Volkov,²⁴ E. Vznuzdaev,³⁸ X. R. Wang,¹³ Y. Watanabe,^{39,40} S. N. White,⁵ F. K. Wohn,¹⁷ C. L. Woody,⁵ W. Xie,⁶ Y. Yang,⁷ A. Yanovich,¹⁵ S. Yokkaichi,^{39,40} G. R. Young,³⁶ I. E. Yushmanov,²⁴ W. A. Zajc,^{9,†} C. Zhang,⁹ S. Zhou,⁷ S. J. Zhou,⁵² and L. Zolin¹⁸

(PHENIX Collaboration)

¹Abilene Christian University, Abilene, Texas 79699, USA

²Institute of Physics, Academia Sinica, Taipei 11529, Taiwan

³Department of Physics, Banaras Hindu University, Varanasi 221005, India

- ⁴Bhabha Atomic Research Centre, Bombay 400 085, India
⁵Brookhaven National Laboratory, Upton, New York 11973-5000, USA
⁶University of California - Riverside, Riverside, California 92521, USA
⁷China Institute of Atomic Energy (CIAE), Beijing, People's Republic of China
⁸Center for Nuclear Study, Graduate School of Science, University of Tokyo, 7-3-1 Hongo, Bunkyo, Tokyo 113-0033, Japan
⁹Columbia University, New York, New York 10027, USA and Nevis Laboratories, Irvington, New York 10533, USA
¹⁰Dapnia, CEA Saclay, F-91191, Gif-sur-Yvette, France
¹¹Debrecen University, H-4010 Debrecen, Egyetem tér 1, Hungary
¹²Florida State University, Tallahassee, Florida 32306, USA
¹³Georgia State University, Atlanta, Georgia 30303, USA
¹⁴Hiroshima University, Kagamiyama, Higashi-Hiroshima 739-8526, Japan
¹⁵IHEP Protvino, State Research Center of Russian Federation, Institute for High Energy Physics, Protvino, 142281, Russia
¹⁶University of Illinois at Urbana-Champaign, Urbana, Illinois 61801, USA
¹⁷Iowa State University, Ames, Iowa 50011, USA
¹⁸Joint Institute for Nuclear Research, 141980 Dubna, Moscow Region, Russia
¹⁹KAERI, Cyclotron Application Laboratory, Seoul, South Korea
²⁰Kangnung National University, Kangnung 210-702, South Korea
²¹KEK, High Energy Accelerator Research Organization, Tsukuba, Ibaraki 305-0801, Japan
²²KFKI Research Institute for Particle and Nuclear Physics of the Hungarian Academy of Sciences (MTA KFKI RMKI), H-1525 Budapest 114, PO Box 49, Budapest, Hungary
²³Korea University, Seoul, 136-701, Korea
²⁴Russian Research Center "Kurchatov Institute," Moscow, Russia
²⁵Kyoto University, Kyoto 606-8502, Japan
²⁶Laboratoire Leprince-Ringuet, Ecole Polytechnique, CNRS-IN2P3, Route de Saclay, F-91128, Palaiseau, France
²⁷Lawrence Livermore National Laboratory, Livermore, California 94550, USA
²⁸Los Alamos National Laboratory, Los Alamos, New Mexico 87545, USA
²⁹LPC, Université Blaise Pascal, CNRS-IN2P3, Clermont-Fd, 63177 Aubiere Cedex, France
³⁰Department of Physics, Lund University, Box 118, SE-221 00 Lund, Sweden
³¹Institut für Kernphysik, University of Muenster, D-48149 Muenster, Germany
³²Myongji University, Yongin, Kyonggido 449-728, Korea
³³Nagasaki Institute of Applied Science, Nagasaki-shi, Nagasaki 851-0193, Japan
³⁴University of New Mexico, Albuquerque, New Mexico 87131, USA
³⁵New Mexico State University, Las Cruces, New Mexico 88003, USA
³⁶Oak Ridge National Laboratory, Oak Ridge, Tennessee 37831, USA
³⁷IPN-Orsay, Université Paris Sud, CNRS-IN2P3, BP1, F-91406, Orsay, France
³⁸PNPI, Petersburg Nuclear Physics Institute, Gatchina, Leningrad Region, 188300, Russia
³⁹RIKEN, The Institute of Physical and Chemical Research, Wako, Saitama 351-0198, Japan
⁴⁰RIKEN BNL Research Center, Brookhaven National Laboratory, Upton, New York 11973-5000, USA
⁴¹Saint Petersburg State Polytechnic University, St. Petersburg, Russia
⁴²Instituto de Física, Universidade de São Paulo, Caixa Postal 66318, São Paulo CEP05315-970, Brazil
⁴³System Electronics Laboratory, Seoul National University, Seoul, South Korea
⁴⁴Chemistry Department, Stony Brook University, SUNY, Stony Brook, New York 11794-3400, USA
⁴⁵Department of Physics and Astronomy, Stony Brook University, SUNY, Stony Brook, New York 11794, USA
⁴⁶SUBATECH (Ecole des Mines de Nantes, CNRS-IN2P3, Université de Nantes) BP 20722 - 44307, Nantes, France
⁴⁷University of Tennessee, Knoxville, Tennessee 37996, USA
⁴⁸Department of Physics, Tokyo Institute of Technology, Oh-okayama, Meguro, Tokyo, 152-8551, Japan
⁴⁹Institute of Physics, University of Tsukuba, Tsukuba, Ibaraki 305, Japan
⁵⁰Vanderbilt University, Nashville, Tennessee 37235, USA
⁵¹Waseda University, Advanced Research Institute for Science and Engineering, 17 Kikui-cho, Shinjuku-ku, Tokyo 162-0044, Japan
⁵²Weizmann Institute, Rehovot 76100, Israel
⁵³Yonsei University, IPAP, Seoul 120-749, Korea

(Received 26 January 2006; published 22 May 2006)

Inclusive transverse momentum spectra of η mesons have been measured within $p_T = 2\text{--}10$ GeV/ c at midrapidity by the PHENIX experiment in Au + Au collisions at $\sqrt{s_{NN}} = 200$ GeV. In central Au + Au the η yields are significantly suppressed compared to peripheral Au + Au, $d + Au$, and $p + p$ yields scaled by the corresponding number of nucleon-nucleon collisions. The magnitude, centrality, and p_T dependence of the suppression is common, within errors, for η and π^0 . The ratio of η to π^0 spectra at high p_T amounts to $0.40 < R_{\eta/\pi^0} < 0.48$ for the three systems, in agreement with the world average measured in hadronic and nuclear reactions and, at large scaled momentum, in e^+e^- collisions.

The major motivation for the study of high energy nucleus-nucleus ($A + A$) collisions is the opportunity to probe strongly interacting matter at extremely high energy densities. Of particular interest are energy densities well above the expected transition from normal hadronic matter to a deconfined system of quarks and gluons. Lattice quantum chromodynamics (QCD) calculations [1] predict that this transition will occur at a temperature of $T \approx 170 \text{ MeV} \approx 10^{12} \text{ K}$. The formation of a quark-gluon plasma (QGP) in $A + A$ reactions should manifest itself in a variety of experimental signatures [2].

At center-of-mass energies reached by the Relativistic Heavy Ion Collider (RHIC), arguably the most exciting experimental results so far are connected with the predicted “jet quenching” phenomenon [3–5] due to energy loss of hard-scattered partons as they traverse the dense medium formed in the reaction. Since (leading) hadrons with $p_T > 4 \text{ GeV}/c$ at RHIC carry a large fraction of the momentum of the parent quark or gluon [$\langle z \rangle = p_{\text{hadron}}/p_{\text{parton}} \approx 0.5\text{--}0.7$ [6,7]], parton energy loss results in a significantly suppressed production of high- p_T hadrons [4]. The inclusive spectra of high- p_T neutral pions [8,9] and charged hadrons [10,11] in Au + Au at $\sqrt{s_{NN}} = 200 \text{ GeV}$ are indeed suppressed by as much as a factor of 5 compared to the corresponding yields in $p + p$ [12] and $d + Au$ [13,14], scaled by the number of incoherent nucleon-nucleon (NN) collisions. The centrality [15], p_T [16–18] and center-of-mass energy [19] dependences of the observed quenching are consistent with theoretical calculations of QCD energy loss due to multiple gluon emission in a dense medium. Assuming a thermalized parton system, the magnitude of the suppression for central Au + Au at $\sqrt{s_{NN}} = 200 \text{ GeV}$ implies initial energy densities above $15 \text{ GeV}/\text{fm}^3$, ~ 100 times larger than normal nuclear matter [20].

The equal amount of suppression for π^0 and h^\pm observed above $p_T \approx 5 \text{ GeV}/c$ for the same Au + Au centrality seems to indicate that the mechanism of quenching is independent of the identity of the high- p_T light-quark hadron. This is expected if the suppression takes place at the parton level *prior* to its fragmentation into a given hadron. Indeed, in this case the high- p_T deficit depends only on the energy lost in the medium by the parent (u, d, s) quark or gluon and not on the nature of the final leading hadron which will be produced with the same *universal* probabilities (fragmentation functions) which govern hadron production in the vacuum in more elementary systems. The partons involved in high- p_T hadroproduction considered in this work have typical momenta $\gtrsim 5 \text{ GeV}/c$, 10 times larger than the “bulk” average momenta $\langle p_T \rangle \approx 0.55 \text{ GeV}/c$ of the system [21]. Such energetic partons are then supposed to traverse (and lose energy in) the medium and hadronize in the *vacuum* a few tens of fm/ c later [15]. The equal suppression of h^\pm and π^0 does not by itself provide a conclusive argument for parton energy loss *before* fragmentation in the vacuum because above $p_T \approx$

$5 \text{ GeV}/c$, unidentified charged hadron yields are dominated by π^\pm [11]. Measurement of the yields of an additional light-quark species like the η meson at large enough p_T allows a confirmation of the independence of the quenching with respect to the nature of the produced hadron, and tests the consistency of the data with medium-induced *partonic* energy loss prior to vacuum hadronization. Besides its interest as a *signal* in its own right, the η meson constitutes, after the π^0 , the second most important source of decay e^\pm and γ . Reliable knowledge of their production cross sections is thus required in order to eliminate the *background* of secondary e^\pm and γ in single electron [22], dielectron [23], and direct γ [24] measurements.

This Letter presents measurements of the η meson by the PHENIX experiment [25] in Au + Au collisions at $\sqrt{s_{NN}} = 200 \text{ GeV}$ during the second RHIC run (2001–2002) and compares them to η from $p + p$ and $d + Au$ [26] and to π^0 [8,9] and direct γ [24] from Au + Au, all measured in the same experiment at the same $\sqrt{s_{NN}}$. The η measurement reaches the second largest p_T for identified hadrons at RHIC, after the π^0 . The analysis reported here uses beam-beam counters (BBC, $3.0 < |\eta| < 3.9$) plus the zero degree calorimeters (ZDC) for trigger and global event characterization. For each collision, the reaction centrality is obtained by cuts in the correlated distribution of the charge detected in the BBC and the energy measured in the ZDC [27]. A Glauber Monte Carlo model combined with a simulation of BBC and ZDC responses is used to determine the corresponding nuclear overlap function $\langle T_{AA} \rangle$ for each centrality [8]. The η mesons are reconstructed at midrapidity in the lead-scintillator (PbSc) electromagnetic calorimeter [28] via their $\gamma\gamma$ decay mode (BR = 39.43%). The PbSc consists of 15 552 individual lead-scintillator sandwich modules ($5.54 \text{ cm} \times 5.54 \text{ cm} \times 37.5 \text{ cm}$, $18 X_0$), grouped in six sectors located at a radial distance of 5.1 m from the beam line, covering a total solid angle of $\Delta\eta \approx 0.7$ and $\Delta\phi \approx 3\pi/4$ rad. The energy calibration of the PbSc modules is obtained from the beam-test values and confirmed with the measured position of the π^0 mass peak, the energy deposited by minimum ionizing particles traversing the calorimeter, as well as with the expected $E_{\text{PbSc}}/p_{\text{tracking}} \sim 1$ value for e^\pm identified by the Ring-Imaging Čerenkov detector. The systematic error on the absolute energy scale is less than 1.5%, which translates into a maximum 8% uncertainty in the final η yields.

For this analysis a minimum bias (MB) trigger sample of 34×10^6 events, also used for the previously published π^0 analysis [8], is combined with a Level-2 trigger event sample for centralities 0%–60%, equivalent to an additional 30×10^6 minimum bias events. The Level-2 trigger sample is obtained with a software trigger on highly energetic particles (3.5 GeV threshold). The resulting trigger reaches a 50% (100%) efficiency for η above $p_T = 5(7) \text{ GeV}/c$. The normalization of the Level-2 data sample

relative to the MB data sample is accurate to 2%. Both sets of events are required to have a vertex position $|z| < 30$ cm along the beam axis. Photon candidates are identified in the PbSc by applying particle identification (PID) cuts based on the time-of-flight and shower profile [8,26]. The systematic uncertainty on the yields related to the applied PID cuts is $\sim 8\%$. The η yields are determined by an invariant mass analysis of photon pairs with asymmetries $|E_{\gamma 1} - E_{\gamma 2}|/(E_{\gamma 1} + E_{\gamma 2}) < 0.5$. The combinatorial background is obtained by combining uncorrelated photon pairs from different events with similar centrality and vertex, and by normalizing the distribution in a region below ($m_{\text{inv}} = 400\text{--}450$ MeV/ c^2) and above ($m_{\text{inv}} = 750\text{--}1000$ MeV/ c^2) the η mass peak. The resulting distribution is fit to a Gaussian plus an exponential to account for the residual background not described by the mixed-event background (inset of Fig. 1). The open (solid) symbols depict the η signal after mixed (plus residual) background subtraction. To estimate the uncertainty in the subtraction procedure, different pair asymmetries and an alternative linear parametrization of the residual background are used. The signal-to-background ratio in peripheral (central) collisions is approximately 1.3 (1.5) for the highest p_T and 0.05 (0.002) for the lowest p_T .

The raw spectra are normalized to one unit of rapidity and full azimuth. This purely geometrical acceptance factor amounts to ~ 4 at large p_T . The spectra are further corrected for the detector response (energy resolution, dead

areas), the reconstruction efficiency (analysis cuts), and occupancy effects (cluster overlaps). These corrections are quantified by embedding simulated single η from a full PHENIX GEANT [29] simulation into real events, and analyzing the merged events with the same analysis cuts used to obtain the real yields. The total η yield efficiency correction is ~ 3 and rises $\leq 20\%$ with centrality. The losses are dominated by fiducial and asymmetry cuts. The nominal energy resolution is adjusted in the simulation by adding a p_T -independent energy smearing of 3% for each PbSc tower. The shape, position, and width of the η peak measured for all p_T 's and centralities are well reproduced by the embedded data.

The main sources of systematic errors in the measurement are the uncertainties in the yield extraction (10%–30%), the yield correction (10%), and the energy scale (a maximum of 8%). The final combined systematic errors on the spectra are at the level of 10%–30% (point-to-point) and 10%–20% (p_T -correlated) depending on the p_T and centrality bin [26]. A correction in the yield to account for the true mean value of each p_T bin is applied to the steeply falling spectra. The fully corrected p_T distributions are shown in Fig. 1 for MB and 3 centrality bins (0%–20%, 20%–60%, and 60%–92%) scaled for clarity by the factors indicated. The error bars are the quadratic sum of statistical and systematic errors.

Medium effects in $A + A$ collisions are quantitatively determined using the *nuclear modification factor* given as the ratio of the measured $A + A$ invariant yield over the $p + p$ cross section scaled by the Glauber nuclear overlap function $\langle T_{AA} \rangle$ in the centrality bin under consideration:

$$R_{AA}(p_T) = \frac{d^2 N_{AA}/dp_T dy}{\langle T_{AA} \rangle d^2 \sigma_{pp}/dp_T dy}. \quad (1)$$

Deviations from $R_{AA}(p_T) = 1$ quantify the degree of departure of the hard $A + A$ yields from an incoherent superposition of NN collisions. Figure 2 compares the nuclear modification factor for η in central (0%–20%), semicentral (20%–60%), and peripheral (60%–92%) Au + Au reactions using the reference $d^2 \sigma_{pp}/dp_T dy$ spectrum measured in $p + p$ collisions [26]. As observed for high- p_T π^0 [8,9], the η yields are consistent with the expectation of independent NN scatterings in peripheral reactions ($R_{AA} \approx 1$) but are increasingly reduced for smaller centralities. The p_T dependence of R_{AA} is flat above 4 GeV/ c as seen also for the π^0 .

Figure 3 compares the $R_{AA}(p_T)$ measured in Au + Au at $\sqrt{s_{NN}} = 200$ GeV for η (0%–20% centrality), π^0 [8,9], and γ [24] (0%–10% centralities). Whereas direct γ are unsuppressed compared to the T_{AA} -scaled reference given here by a next-to-leading-order (NLO) calculation [24,30] that reproduces the PHENIX $p + p$ photon data well [31], π^0 and η are suppressed by a similar factor of ~ 5 compared to the corresponding $p + p$ cross sections [9,26]. Within the current uncertainties, light-quark mesons at

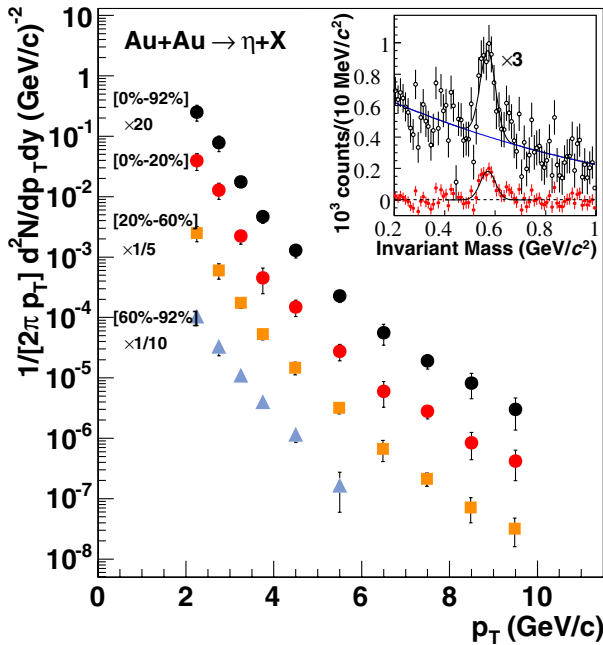


FIG. 1 (color online). Invariant η yields as a function of transverse momentum for 3 centralities and MB Au + Au at $\sqrt{s_{NN}} = 200$ GeV scaled by the factors indicated in the plot. Inset: invariant mass distribution of γ pairs with $p_T = 4\text{--}5$ GeV/ c measured in MB Au + Au, after mixed-event (black open circles) plus residual (red solid circles) background subtraction.

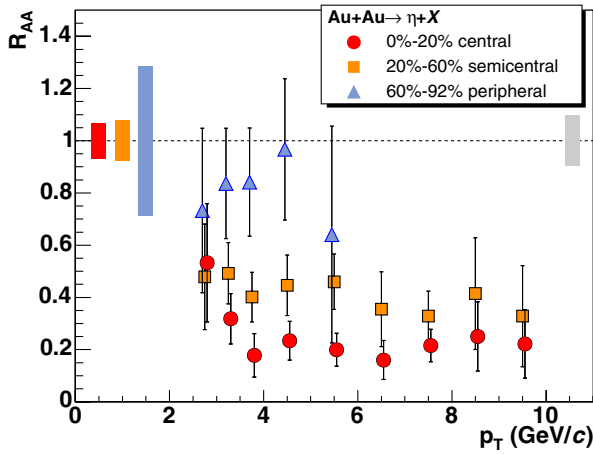


FIG. 2 (color online). Nuclear modification factors for η in Au + Au centralities: 0%–20%, 20%–60%, 60%–92%. The error bars show point-to-point uncertainties. The absolute normalization error bands at $R_{AA} = 1$ show the uncertainties in $\langle T_{AA} \rangle$ for decreasing centralities. The error box on the right indicates the 9.7% $p + p$ cross-section uncertainty [14].

RHIC show a flat suppression in the range $p_T = 4$ –14 GeV/c, independent of their mass (note that the η is 4 times heavier than the π^0). The results are in agreement with expectations of in-medium non-Abelian energy loss of the parent parton prior to its fragmentation in the vacuum. The initial gluon densities needed to quench the high- p_T hadrons by such an amount are of the order of $dN^s/dy = 1100$ (solid curve in Fig. 3) [16].

An additional way to determine possible differences in the suppression pattern of π^0 and η is to study the centrality dependence of the η/π^0 ratio in Au + Au collisions

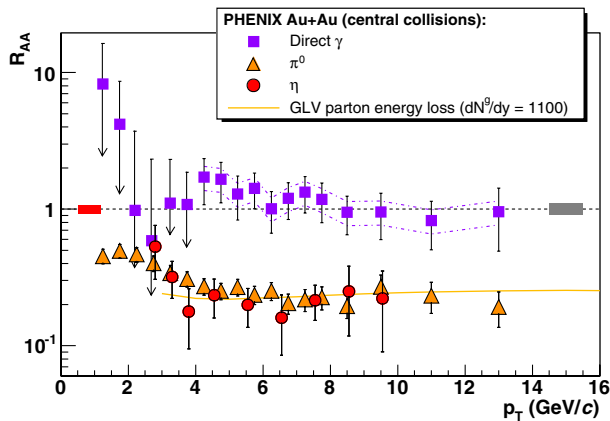


FIG. 3 (color online). $R_{AA}(p_T)$ measured in central Au + Au at $\sqrt{s_{NN}} = 200$ GeV for η , π^0 [8,9], and direct γ [24]. The error bars include all point-to-point errors. The error bands at $R_{AA} = 1$ have the same meaning as in Fig. 2. The baseline $p + p \rightarrow \gamma + X$ reference used is a NLO calculation [24,30], that reproduces our own data well [31], with theoretical uncertainties indicated by the dash-dotted lines around the points. The solid yellow curve is a parton energy loss prediction for a medium with density $dN^s/dy = 1100$ [16].

and compare it with the ratio in more elementary systems (e^+e^- , $p + p$, $d + Au$). The η/π^0 ratio in hadron-hadron, hadron-nucleus, and nucleus-nucleus collisions is seen to increase rapidly with p_T and flatten out above $p_T \approx 2.5$ GeV/c at an asymptotically constant $R_{\eta/\pi^0} \approx 0.5$ for all systems [26]. Likewise, in e^+e^- at the Z pole ($\sqrt{s} = 91.2$ GeV) one also finds $R_{\eta/\pi^0} \approx 0.5$ for η and π^0 at large scaled momenta $x_p = p_{\text{hadron}}/p_{\text{beam}} \gtrsim 0.3$ –0.7 [26] consistent with the range of fractional momenta $\langle z \rangle$ relevant for high- p_T production discussed here. It is interesting to test if this ratio is modified in any way by final- and/or initial-state medium effects in Au + Au collisions at RHIC.

Figure 4 shows $R_{\eta/\pi^0}(p_T)$ for three Au + Au centrality selections and for $p + p$ and $d + Au$ collisions [26]. A fit to a constant for $p_T > 2$ GeV/c gives $R_{\eta/\pi^0}^{\text{AuAu}0\%-20\%} = 0.40 \pm 0.04$, $R_{\eta/\pi^0}^{\text{dAuMB}} = 0.47 \pm 0.03$, and $R_{\eta/\pi^0}^{\text{pp}} = 0.48 \pm 0.03$, where the quoted errors are the quadratic sum of statistical and systematic uncertainties. The Au + Au ratio is consistent within $\sim 1\sigma$ with both the essentially identical $d + Au$ and $p + p$ ratios. The R_{η/π^0} ratio shows thus no apparent collision system, centrality, or p_T dependence. The dotted curve is the predicted PYTHIA [32] result for the $p + p$ ratio at $\sqrt{s} = 200$ GeV which is also coincident with the world data measured in the same momentum range in hadronic, nuclear, and e^+e^- collisions in a wide range of energies ($\sqrt{s} \approx 3$ –1800 GeV) [26].

In summary, the transverse momentum spectra of η mesons have been measured at midrapidity in the range $p_T = 2$ –10 GeV/c in Au + Au at $\sqrt{s_{NN}} = 200$ GeV. The invariant yields per nucleon-nucleon collision are increasingly depleted with centrality in comparison to $p + p$ results at the same center-of-mass energy. The maximum

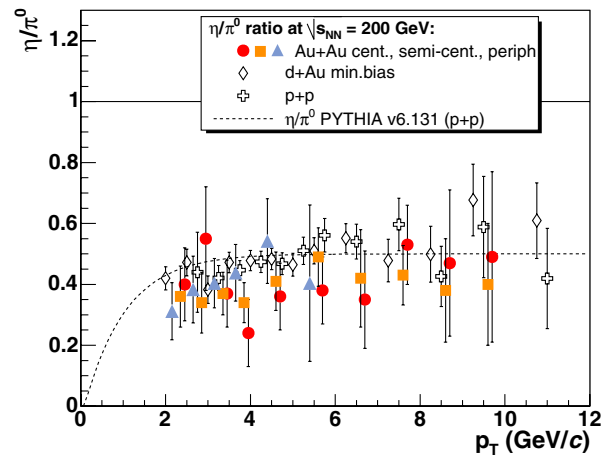


FIG. 4 (color online). η/π^0 ratio in Au + Au (centralities: 0%–20%, 20%–60%, 60%–92%) compared to the ratio in $p + p$ and $d + Au$ [26] at $\sqrt{s_{NN}} = 200$ GeV. The error bars include all point-to-point errors that do not cancel in the ratio of yields. The dashed curve is the PYTHIA [32] prediction for $p + p$ at $\sqrt{s} = 200$ GeV consistent with the asymptotic $R_{\eta/\pi^0} \approx 0.5$ measured in hadronic and e^+e^- collisions in a wide range of c.m. energies [26].

suppression factor is ~ 5 in central Au + Au. The magnitude, p_T , and centrality dependences of the suppression are the same for η and π^0 suggesting that the production of light neutral mesons at large p_T in nuclear collisions at RHIC is affected by the medium in the same way. The measured η/π^0 ratio is flat with p_T and amounts to $R_{\eta/\pi^0} = 0.40 \pm 0.04$. This value is consistent with the world value at high p_T in hadronic and nuclear reactions and, at high x_p , in e^+e^- collisions. We conclude that all these observations are in agreement with a scenario where the parent parton first loses energy in the produced dense medium and then fragments into a leading meson in the vacuum according to the same probabilities that govern high- p_T hadroproduction in more elementary systems ($p + p$, e^+e^-).

We thank the staff of the Collider-Accelerator and Physics Departments at BNL for their vital contributions. We acknowledge support from the Department of Energy and NSF (USA), MEXT and JSPS (Japan), CNPq and FAPESP (Brazil), NSFC (China), CNRS-IN2P3 and CEA (France), BMBF, DAAD, and AvH (Germany), OTKA (Hungary), DAE and DST (India), ISF (Israel), KRF and CHEP (Korea), RMIST, RAS, and RMAE (Russia), VR and KAW (Sweden), US CRDF for the FSU, US-Hungarian NSF-OTKA-MTA, and US-Israel BSF.

*Deceased.

†PHENIX Spokesperson.

Email address: zajc@nevis.columbia.edu

- [1] F. Karsch, Lect. Notes Phys. **583**, 209 (2002).
 [2] J. W. Harris and B. Müller, Annu. Rev. Nucl. Part. Sci. **46**, 71 (1996).
 [3] J. D. Bjorken, Fermilab Report No. FERMILAB-PUB-82-059-THY, 1982 (unpublished).
 [4] M. Gyulassy and M. Plümer, Phys. Lett. B **243**, 432 (1990); X. N. Wang and M. Gyulassy, Phys. Rev. Lett. **68**, 1480 (1992).
 [5] R. Baier, Y. L. Dokshitzer, A. H. Mueller, S. Peigné, and D. Schiff, Nucl. Phys. **B484**, 265 (1997); R. Baier, D. Schiff, and B. G. Zakharov, Annu. Rev. Nucl. Part. Sci. **50**, 37 (2000); U. Wiedemann, Nucl. Phys. **B588**, 303 (2000).
 [6] S. S. Adler *et al.* (PHENIX Collaboration), hep-ex/0605039 (to be published).
 [7] S. Kretzer, Acta Phys. Pol. B **36**, 179 (2005).
 [8] S. S. Adler *et al.* (PHENIX Collaboration), Phys. Rev. Lett. **91**, 072301 (2003).
 [9] S. S. Adler *et al.* (PHENIX Collaboration) (to be published).
 [10] J. Adams *et al.* (STAR Collaboration), Phys. Rev. Lett. **91**, 172302 (2003).
 [11] S. S. Adler *et al.* (PHENIX Collaboration), Phys. Rev. C **69**, 034910 (2004).
 [12] S. S. Adler *et al.* (PHENIX Collaboration), Phys. Rev. Lett. **91**, 241803 (2003).
 [13] S. S. Adler *et al.* (PHENIX Collaboration), Phys. Rev. Lett. **91**, 072303 (2003).
 [14] S. S. Adler *et al.* (PHENIX Collaboration) (to be published).
 [15] X. N. Wang, Phys. Lett. B **579**, 299 (2004).
 [16] I. Vitev and M. Gyulassy, Phys. Rev. Lett. **89**, 252301 (2002); I. Vitev, J. Phys. G **30**, S791 (2004).
 [17] K. J. Eskola, H. Honkanen, C. A. Salgado, and U. A. Wiedemann, Nucl. Phys. **A747**, 511 (2005).
 [18] S. Jeon and G. D. Moore, Phys. Rev. C **71**, 034901 (2005).
 [19] D. d'Enterria, Eur. Phys. J. C **43**, 295 (2005).
 [20] K. Adcox *et al.* (PHENIX Collaboration), Nucl. Phys. **A757**, 184 (2005).
 [21] S. S. Adler *et al.* (PHENIX Collaboration), Phys. Rev. C **69**, 034909 (2004).
 [22] K. Adcox *et al.* (PHENIX Collaboration), Phys. Rev. Lett. **88**, 192303 (2002); S. S. Adler *et al.* (PHENIX Collaboration), Phys. Rev. C **72**, 024901 (2005); Phys. Rev. Lett. **96**, 032301 (2006).
 [23] A. Toia (PHENIX Collaboration), *Proceedings of the QM'05*, nucl-ex/0510006.
 [24] S. S. Adler *et al.* (PHENIX Collaboration), Phys. Rev. Lett. **94**, 232301 (2005).
 [25] K. Adcox *et al.* (PHENIX Collaboration), Nucl. Instrum. Methods Phys. Res., Sect. A **499**, 469 (2003).
 [26] S. S. Adler *et al.* (PHENIX Collaboration) (to be published).
 [27] K. Adcox *et al.* (PHENIX Collaboration), Phys. Rev. Lett. **86**, 3500 (2001).
 [28] L. Aphecetche *et al.* (PHENIX Collaboration), Nucl. Instrum. Methods Phys. Res., Sect. A **499**, 521 (2003).
 [29] F. Carminati *et al.*, *GEANT 3.21: Detector Description and Simulation Tool*, CERN Program Library Long Writeup No. W5013, 1993 (unpublished).
 [30] L. E. Gordon and W. Vogelsang, Phys. Rev. D **48**, 3136 (1993); Phys. Rev. D **50**, 1901 (1994).
 [31] S. S. Adler *et al.* (PHENIX Collaboration), Phys. Rev. D **71**, 071102 (2005); K. Okada (PHENIX Collaboration), *Proceedings of SPIN04*, hep-ex/0501066.
 [32] T. Sjöstrand, Comput. Phys. Commun. **82**, 74 (1994); computer code PYTHIA v6.131 with default parameters.